

1 **Spatiotemporal variation in Oregon salt marsh expansion and contraction**

2 **Erin K. Peck^{1,2} & Robert. A. Wheatcroft¹**

3 ¹Oregon State University, College of Earth, Ocean, & Atmospheric Sciences, Corvallis, OR
4 97331, USA (EKP: peckerin@oregonstate.edu; RAW: rob.wheatcroft@oregonstate.edu)

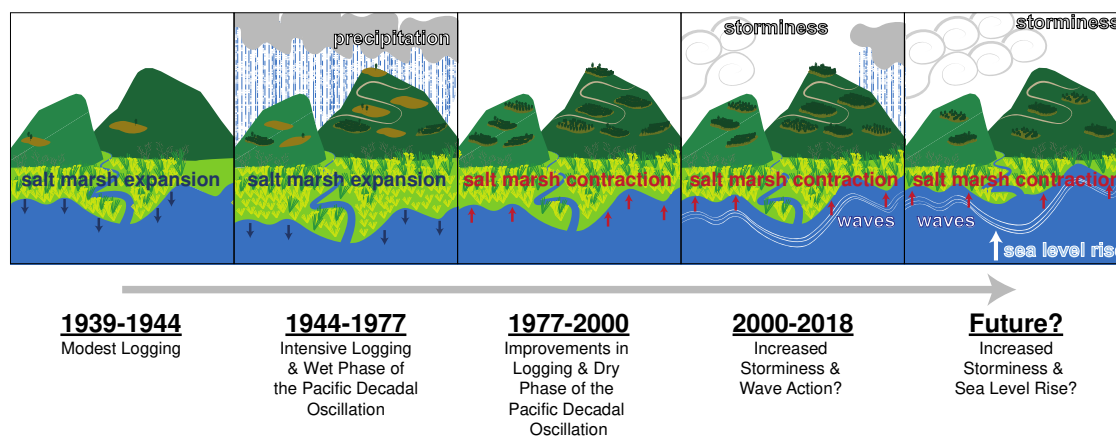
5 ²University of Delaware, Plant and Soil Sciences, Newark, DE 19716, USA (Present Address)

6 Corresponding author: Erin Peck (peckerin@oregonstate.edu)

7 **Key Words:** salt marshes; geographic information systems; land use; sediment dynamics;
8 morphodynamics; lateral change

9 **Regional Key Words:** USA, Oregon coast

10 **Graphical Abstract**



11

12 **Abstract**

13 Spatiotemporal patterns of salt marsh lateral change vary along the Oregon coast, reflecting
14 complex drivers of marsh morphodynamics. To identify potential factors influencing salt marsh
15 expansion/contraction, time-series (~10 y resolution over ~80 y) of marsh edge position and area
16 were measured from aerial imagery in five Oregon estuaries with variable morphologies, fluvial
17 sediment supplies, relative sea level change, and vertical accretion rates. In estuaries where there
18 exists room for marsh growth onto unvegetated tidal flats, net lateral expansion occurs when
19 vertical accommodation space is filled and under relatively high sediment supplies. Moreover,
20 results suggest that conditions promoting elevated sediment supply in the mid-20th century –
21 intensive timber harvest coincident with increased precipitation during the wet phase of the
22 Pacific Decadal Oscillation (PDO) – caused marsh expansion. In the late 20th century, rates of
23 expansion have slowed, sometimes giving way to net contraction; conditions favoring slowed
24 sediment supply – reduced timber harvest and improved logging methods combined with
25 reduced precipitation/discharge during the dry phase of the PDO – are likely culprits. More
26 recently, edges continued to contract possibly forecasting vulnerability under future accelerated
27 sea level rise. In addition to providing rates of salt marsh expansion/contraction for an
28 understudied portion of the US coastline, these results highlight the importance of considering
29 current salt marsh trajectories in the context of past land use and time-varying hydroclimate.

30 **1 Introduction**

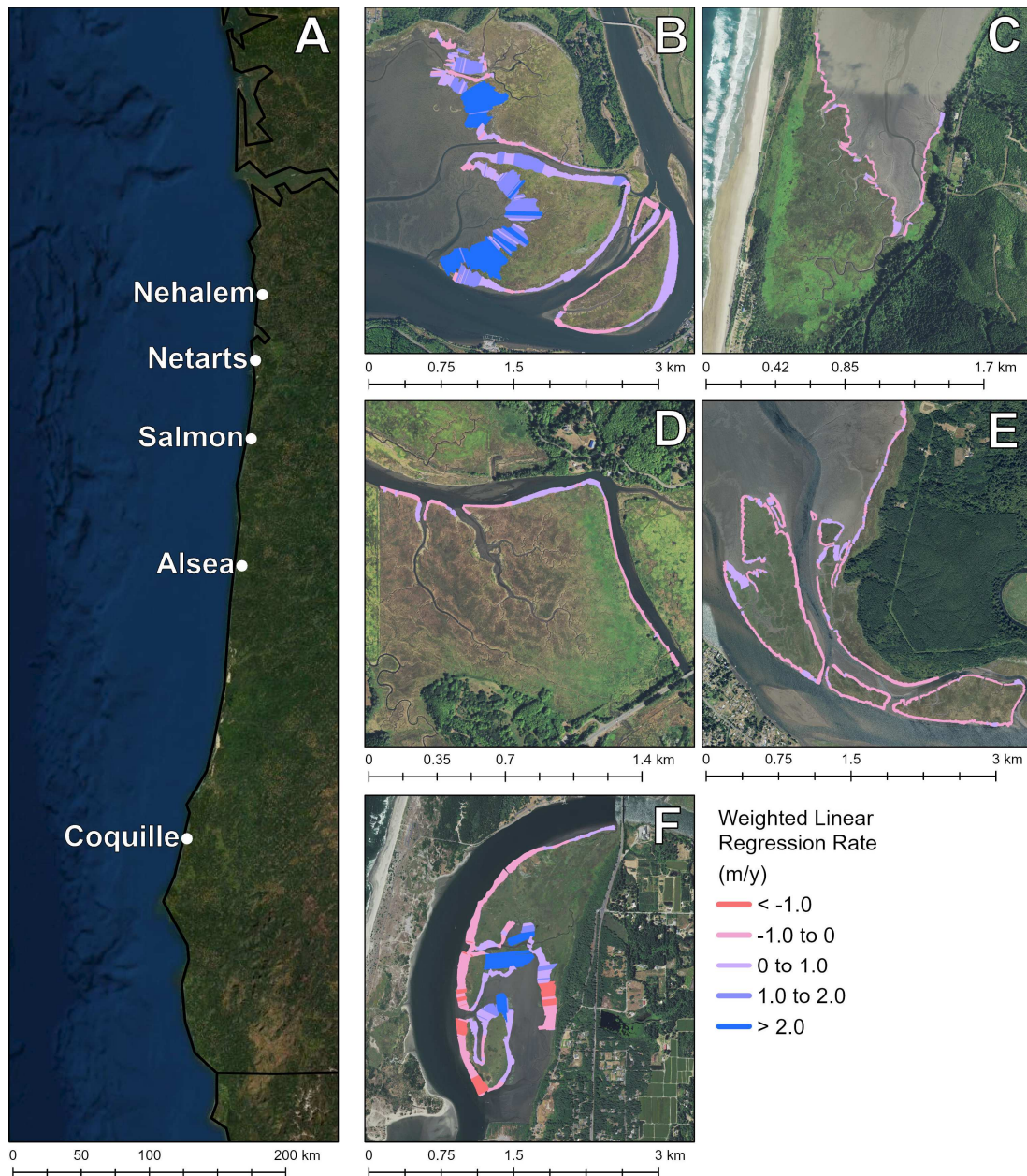
31 Salt marshes provide numerous ecosystem services, including flood protection, habitat,
32 and carbon burial (Barbier et al., 2011), yet are increasingly threatened by climate and land-use
33 changes (Gedan et al., 2009; Weston, 2014). As such, determining rates and mechanisms of salt
34 marsh vertical accretion and lateral expansion/contraction is of great importance, especially for
35 the parameterization of models that can predict the futures of coastal ecosystems and their
36 services (Fagherazzi et al., 2020; Wiberg et al., 2020). Salt marsh vertical accretion – a product
37 of accommodation space created by relative sea level rise, sediment supplied to the marsh
38 platform, and autochthonous organic matter accumulation – has long been assessed as a measure
39 of salt marsh vulnerability to drowning (Redfield, 1972). However, focus on vertical rates of
40 change may neglect that lateral expansion/contraction contributes to the overall size of the salt
41 marsh platform, and marshes may be particularly vulnerable to edge contraction more so than
42 elevation loss (Kirwan, Temmerman, et al., 2016). More measurements of lateral rates and
43 drivers of change are required to improve understanding of whole-platform morphodynamics,
44 especially as empirical studies of lateral dynamics have lagged behind mechanistic investigations
45 (Ladd et al., 2019). Lateral contraction at the marsh-tidal flat boundary is primarily a product of
46 edge erosion, which occurs through wave attack exacerbated by increased water levels (a product
47 of relative sea level rise, increased storminess, and fluvial discharge; Mariotti & Carr, 2014;
48 Mariotti & Fagherazzi, 2010). Edge erosion may deliver sediment to starved platforms and
49 simultaneous migration into adjacent upland forests may maintain overall salt marsh extent (e.g.,
50 Mariotti & Carr, 2014; Kirwan, Walters, et al., 2016; Carr et al., 2020; Ganju et al., 2020).
51 Conversely, progradation has been observed to occur under high sediment supplies (Ladd et al.,
52 2019), though examples of lateral expansion are less common, especially in estuarine systems of

53 US East and European Coasts (Fagherazzi et al., 2020). However, these assessments have
54 generally focused on sediment-limited systems located on passive margins with wide coastal
55 plains (e.g., the US East Coast; Langston et al., 2020; Molino et al., 2021).

56 Oregon salt marshes, which are under-represented in the global morphodynamic literature
57 (e.g., Kirwan, Temmerman, et al., 2016), may represent valuable end-member examples that
58 provide insight into potentially under-studied drivers of lateral change. This is because Oregon
59 rivers have naturally high sediment loads (Wise, 2018; i.e., creating mineralogenic salt marshes);
60 hydroclimatic variations that result in decadal changes in precipitation and discharge (Wheatcroft
61 et al., 2013); different along-margin rates of sea level change (-1.5 to +2.5 mm y⁻¹; Komar et al.,
62 2011); and variable bay morphologies impacting wave energy, though short fetches likely limit
63 wave attack. Additionally, an ~30 y long period (1944 to 1977) of intensive timber harvest in the
64 Oregon Coast Range coincident with the wet phase of the Pacific Decadal Oscillation (PDO;
65 Andrews & Kutura, 2005; Wheatcroft et al., 2013) offers an excellent opportunity to assess the
66 impacts of increased sediment supply on patterns of salt marsh lateral expansion. How these
67 patterns changed in response to a subsequent ~40 years (1977 to 2018) of reduced logging
68 (Richardson et al., 2018; Wetherell et al., 2021) and shifting hydroclimate (i.e., the PDO
69 predominately in the dry phase) reveals the lasting impact of perturbations on salt marsh
70 sediment accumulation and sediment routing systems, globally relevant to regions that
71 experienced a similar history (e.g., deforestation and damming). Furthermore, assessment of
72 rates and drivers of lateral change along the Oregon coast are important to local stakeholders
73 because these salt marshes may be particularly vulnerable to loss (Thorne et al., 2018). Indeed,
74 independent information indicates that ~85% of U.S. West Coast vegetated tidal wetlands have
75 been lost due to diking and tide gate construction since Euro-American incursion (Brophy et al.,

76 2019). Looking to the future, under accelerated sea level rise, more marsh area might be
77 vulnerable to loss, especially since steep topography associated with the Oregon Coast Range
78 prevents significant landward migration of existing salt marshes, deemed critical to marsh
79 survival (Mariotti & Carr, 2014; Kirwan, Walters, et al., 2016; Carr et al., 2020; Ganju et al.,
80 2020).

81 To assess potential long-term drivers of salt marsh expansion/contraction, we measured
82 lateral growth rates over the last ~80 y in five Oregon estuaries: Nehalem, Netarts, Salmon,
83 Alsea, and Coquille. These systems vary in terms of bay morphology, mean annual fluvial
84 sediment supply, and relative sea level changes, and are relatively unimpacted by early 20th
85 century dikes. The importance of these natural forcings in driving marsh expansion and
86 contraction were assessed by comparing long-term rates of edge change across estuaries. Further,
87 to assess the importance of changing land use and hydroclimate on coastal morphodynamics,
88 roughly decadal rates of salt marsh expansion/contraction were calculated for each estuary.
89 These rates were binned into four distinct periods to assess the relative importance of the PDO
90 and history of timber harvest on salt marsh expansion/contraction. The results elucidate both
91 spatiotemporal patterns of salt marsh lateral morphodynamics and potentially provide insight
92 into future trajectories under changing climate and land-use scenarios.



93

94 **Figure 1.** Oregon Coast (a) and aerial images from the 2018 Oregon Statewide Imagery Program
 95 of salt marshes from each estuary (b-e) Nehalem, Netarts, Salmon, Alsea, and Coquille,
 96 respectively). Colored transects display the rate of lateral salt marsh change from ~1940 to the
 97 present, calculated as the weighted linear regression of ≥ 6 digitized marsh edges with dates
 98 approximately every decade. Red indicates contraction, purple indicates no change, and blue
 99 indicates progradation. Transects are spaced 5 m apart.

100 **Table 1.** Estuary Characteristics

	Nehalem	Netarts	Salmon	Alsea	Coquille ¹⁰¹
Watershed Area (km ²)	2209	42	193	1221	2736
Relative Sea Level Change (mm y ⁻¹)	0.9 ± 1.0	1.5 ± 1.0	2.2 ± 0.9	2.8 ± 0.8	-1.4 ± 0.2
Sediment Load (x 10 ³ t y ⁻¹)	224	2.5	20.1	110	178
Area Normalized Sediment Load (x 10 ³ t km ⁻² y ⁻¹) ^a	56	2.6	30	52	105 103
High Marsh Vertical Accretion Rate (mm y ⁻¹) ^b	2.9 ± 1.0	1.9 ± 0.6	1.6 ± 0.3	1.7 ± 0.4	1.3 ± 0.3 104

^a Sediment load is normalized to the 2018 marsh areas presented in Table S1; ^b from Peck et al., 2020

105

106 **2 Methods**

107 *2.1 Sites & environmental data*

108 The study estuaries (Figure 1) – Nehalem, Netarts, Salmon, Alsea, and Coquille – were
 109 chosen based on access to aerial photographs and variability in potential environmental drivers
 110 (Table 1). Rates of 20th century relative sea level change were previously calculated (Peck et al.,
 111 2020) as the difference in eustatic sea level rise (Mazzotti et al., 2008) and interseismic land
 112 uplift (Burgette et al., 2009). Vertical accretion rates were also previously measured by Peck et
 113 al. (2020) and provide insight into which systems are accumulating sediment faster or slower
 114 (i.e., drowning) than relative sea level rise.

115 Annual mean sediment loads were estimated using the U.S. Geological Survey’s
 116 SPATIally Referenced Regressions On Watershed attributes (SPARROW) model (Wise, 2018),
 117 and were normalized to marsh area. Because time-varying rates of suspended sediment
 118 concentrations are unavailable for these systems, histories of timber harvest and fluvial discharge
 119 were determined as proxies for sediment yield. Volume (i.e., board feet) of timber harvested was
 120 estimated for and normalized to each watershed using county-specific timber harvest data
 121 (Andrews & Kutara, 2005) and the fraction of basin area within each county. Peak annual
 122 discharge and cumulative residual discharge (*sensu* Wheatcroft et al., 2013) were calculated from
 123 long-term (\leq 1939) daily discharge recorded on the Nehalem River near Foss, OR (USGS gauge:

124 14301000), Alsea River near Tidewater, OR (USGS gauge: 14306500), and South Fork of the
125 Coquille River at Powers, OR (USGS gauge: 14325000). Salmon River is not gauged, and
126 Netarts Bay has no major river. Monthly precipitation was determined at each of the stream
127 gauge locations using the Parameter-elevation Regression on Independent Slopes Model
128 (PRISM; Daly et al., 1994).

129 Wave heights and directions are not available for our estuaries of interest, but medium-
130 term (≥ 15 y) hourly wind speed and direction data, which can identify expected hotspots of
131 wave attack, were available for four stations spanning the Oregon coast (Astoria, Tillamook,
132 Newport, and Coos) from NOAA's National Centers for Environmental Information. The wind
133 database was queried for speeds > 10 m s^{-1} .

134 *2.2 Lateral change*

135 Salt marsh lateral change was quantified through comparison of roughly decadal aerial
136 photographs from 1939 to the 1990s (scanned at the University of Oregon's Map & Aerial
137 Photography Library) and 21st century aerial imagery downloaded from the Oregon Statewide
138 Imagery Program (https://www.oregon.gov/geo/Pages/imagery_data.aspx; Table S1 and Figure
139 S1). All images were georeferenced in ArcGIS Pro 2.2 using at least 10 control points and fitted
140 using second-order polynomial transformations (e.g., Schieder et al., 2018). The seaward
141 boundaries of salt marshes were hand digitized from georeferenced aerial photographs, and
142 shoreline position uncertainties were estimated following Ruggiero et al. (2013). We excluded
143 areas of marshes in which dikes or tide gates prevented inundation. To minimize the impact of
144 unknown tidal height during image collection, low-resolution images and those that clearly
145 displayed extensive flooding were excluded, and we focused interpretations on multi-decadal
146 rates of shoreline and area change. Landward edges on fringing marshes were not analyzed as

147 relatively limited rates of 20th century sea level rise have prevented much conversion of coastal
148 forested wetlands to marsh (Brophy & Ewald, 2017). Further, in many areas the steep slopes of
149 the hills that fringe Oregon marshes prevent landward migration.

150 Spatially variable rates of lateral change were calculated using the USGS Digital
151 Shoreline Analysis System (DSAS; Himmelstoss et al., 2018) in ArcMap 10.7.1 over roughly
152 decadal periods from 1939 to 2018 and integrated over the period of record. DSAS automatically
153 placed transects at 5-m intervals perpendicular to digitized marsh edges. When calculating the
154 rate of edge change integrated over all digitized edges, a weighted linear regression was fitted for
155 any transect that passed through ≥ 6 edges (Figure S1). Error estimates associated with the
156 weighted linear regression were calculated with 95% confidence intervals. When calculating the
157 rate of change between each period in DSAS (Table S2; Figure S2), uncertainty was
158 conservatively calculated as the sum of edge position uncertainties (Table S1) divided by the
159 time elapsed between photographs; rate changes less than the uncertainty were considered not
160 significant (i.e., neutral edge change; Figures 1 and S1). To compare the influence of wind waves
161 on edge contraction, weighted linear regression rates of net change were queried for marsh edges
162 lying perpendicular to oncoming winter and summer wind directions (wind directions relative to
163 marsh edges were determined using the 2018 digitizations). Edges perpendicular to oncoming
164 winds $> 10 \text{ m s}^{-1}$ are deemed exposed, and other edges are deemed protected. The mean rates of
165 change were normalized to the percent edge length (rate x (edge exposed/total edge length)).
166 These calculations were made for Nehalem and Alsea as these systems are comparable (similar
167 depths and tidal ranges) and are likely more impacted by wind waves than bays that lack
168 substantial fetch (Salmon and Coquille) or have salt marshes oriented away from the dominant
169 oncoming wind directions (Netarts).

170 To calculate changes in area over time (Table S2), a current estuary extent map (Brophy
171 et al., 2019) was used to create a fixed upslope edge position for the fringing marshes. Area
172 uncertainties were calculated as the square of the position uncertainty. To determine the impact
173 of time-varying hydroclimate and land-use change on marsh morphology, rates of area change
174 were linearly interpolated to annual rates and then binned into four time periods of interest.

175 Spatial resolutions of aerial photographs (0.2 to 1.6 m) and root mean squared errors
176 associated with georeferenced photographs (0.09 to 3.6 m) were consistently low; these values
177 were generally best prior to 1980 and after 2000 (Table S1). As a result, shoreline position
178 uncertainties (1.0 to 3.8 m) and area uncertainties (1.0 to 14 m², equating $\leq 0.1\%$ of total area)
179 were negligible (based conservatively on two significant figures).

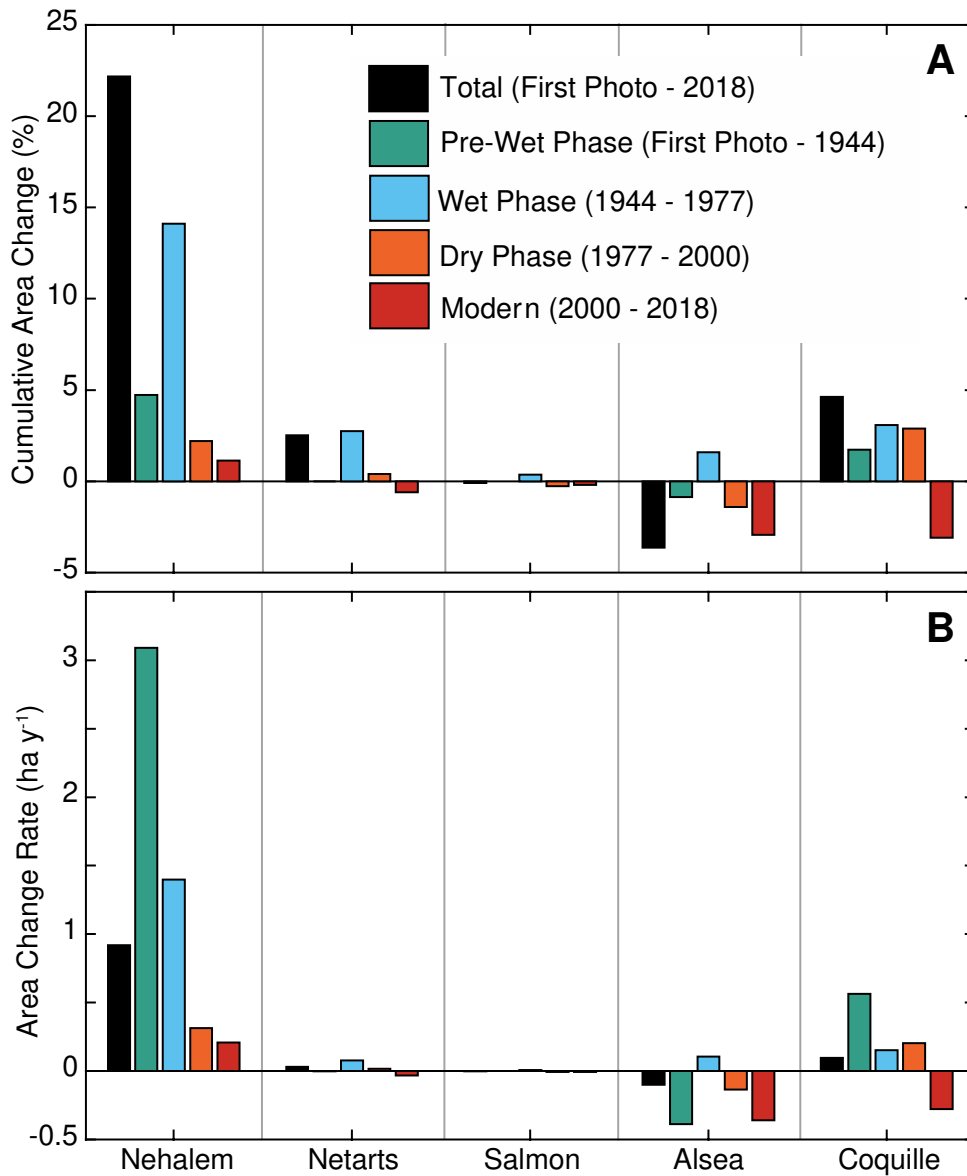
180 **3 Results**

181 *3.1 Temporally Integrated Rates of Lateral Change*

182 Edge change rates integrated over all marsh edges from 1939 to 2018 using weighted
183 linear regression were spatially variable (Figure 1). Coquille salt marshes experienced the fastest
184 rates of net edge contraction and expansion (range = -1.8 to 6.1 m y⁻¹), while Salmon displayed
185 the least amounts of edge change, ranging from -0.27 to 0.24 m y⁻¹. Net rates of edge change
186 ranged from -0.90 to 5.1 m y⁻¹ in Nehalem, from -0.31 to 0.60 m y⁻¹ in Netarts, and from -0.72 to
187 0.92 m y⁻¹ in Alsea.

188 Long-term area change rates, calculated as the difference in areas from the most recent
189 and oldest photograph, revealed spatially integrated lateral fluctuations. Since 1939, Nehalem
190 and Coquille net expanded in area by 22 and 4.6% (73 and 7.5 ha), equivalent to adding 0.92 and
191 0.095 ha y⁻¹, respectively (Figure 2). Netarts and Salmon have shown little net area change in the

192 last ~80 y, having changed by 2.5 and -0.10%, respectively (2.4 and -0.067 ha or 0.030 and -9.2
 193 x 10⁻⁴ ha y⁻¹). Conversely, Alsea net contracted by 3.6% (-8.0 ha), equivalent to -0.10 ha y⁻¹.



194

195 **Figure 2.** Bar plots of (a) cumulative area change and (b) area change rate for the five salt
 196 marshes for the total period of record and binned into five time periods. The first aerial
 197 photograph in all estuaries is 1939 except in Salmon, which is 1945. Salmon is therefore

198 excluded from the pre-wet phase period and the wet phase calculation is 1945 to 1977. Error bars
199 are too small to be visible.

200 *3.2 Temporally Variable Rates of Lateral Change*

201 Each estuary displayed periods of salt marsh area expansion and contraction (Table S1).
202 The fastest period of expansion occurred in Nehalem between 1939 to 1945, with the salt marsh
203 gaining 3 ha y⁻¹ (+19 ha total). Maximal contraction occurred in Coquille from 1942 to 1954,
204 with the salt marsh losing 1.1 ha y⁻¹ (-13 ha total).

205 When divided into four timeframes of interest, consistent patterns emerge along the
206 Oregon coast (Figure 2). From 1939 to 1944, Nehalem and Coquille both added area (4.7 and
207 1.7%, respectively), while Alsea experienced its greatest loss of area (-0.88%), and Netarts did
208 not change (-0.0053%; Salmon salt marsh did not have aerial photographs prior to 1945). From
209 1944 to 1977, all salt marshes gained area (Nehalem:14%, Netarts: 2.7%, Salmon: 0.37%, Alsea:
210 1.6%, Coquille: 3.0%). From 1977 to 2000, cumulative area gain slowed in all systems (2.2,
211 0.39, and 2.9% in Nehalem, Netarts, and Coquille, respectively), with Salmon and Alsea
212 experiencing loss (-0.28 and -1.4%, respectively). From 2000 to 2018, all salt marshes either
213 contracted (-0.60, -0.19, -2.9, and -3.1% in Netarts, Salmon, Alsea, and Coquille, respectively) or
214 experienced the smallest addition of area, as was the case in Nehalem (1.1%).

215 **4 Discussion**

216 Net lateral changes since 1939 are variable amongst the five estuaries highlighting the
217 complexity of salt marsh morphodynamics along the Oregon coast. These net lateral changes
218 agree with earlier literature observations of general patterns of expansion/contraction, which
219 exist for Nehalem (Johannessen, 1964), Coquille (Benner, 1992), and Alsea (Brophy, 1999). In
220 addition to displaying variable net lateral rates of change over the last ~80 y between estuaries,

221 rates of lateral change differed spatially along edges of each salt marsh complex and temporally
222 on decadal timescales. To place these changes in a wider context, we investigate potential spatial
223 and temporal factors influencing expansion/contraction.

224 *4.1 Spatial controls on lateral expansion & contraction*

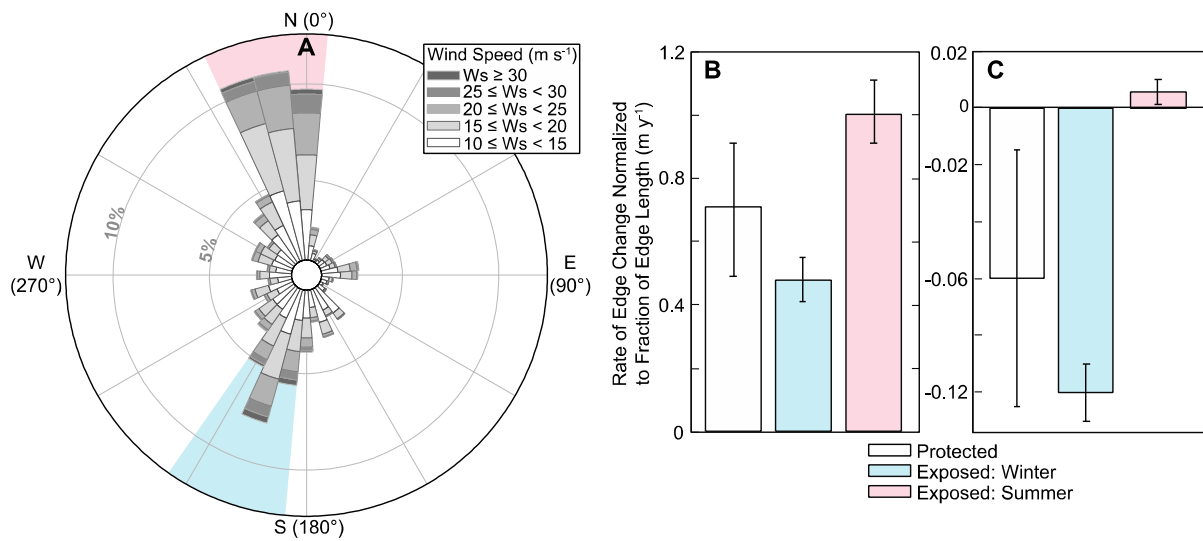
225 Intra-estuary trends in salt marsh expansion/contraction are spatially variable (Figure 1)
226 suggesting internal influencing factors that affect erosion are relevant. In general, edges along
227 river channels are affected by high velocity flows and exhibit the highest rates of contraction. All
228 salt marshes except Netarts, which is not associated with a major channel, are strongly fluvially
229 influenced, and as such are located in the inner side of the river bends where velocities are
230 slowest. Despite being positioned in “point bar” locations, these salt marsh edges all display
231 areas of net contraction potentially as a combined result of high river discharge, tidal action, and
232 wave attack from wind and wakes. For example, Coquille salt marsh displays the highest rates of
233 net contraction (Figure 1F) on its channel edge. Conversely, edges that are protected from high-
234 velocity channel flows appear to exhibit the fastest rates of lateral expansion as is most apparent
235 in Nehalem and Coquille. These rapid rates of expansion are driven in part by relatively high
236 area-normalized annual sediment loads (56 and $105 \times 10^3 \text{ t km}^{-2} \text{ y}^{-1}$, respectively; Table 1), as
237 others have observed to be important elsewhere (e.g., Ladd et al., 2019). Rapid rates of spatially
238 variable lateral expansion are, however, absent from the other systems. Low fluvial sediment
239 inputs to Netarts limits edge expansion, while the lack of space (e.g., tidal flat or subtidal areas)
240 in Salmon restricts growth.

241 The reasons for Alsea’s lack of lateral expansion and net contraction are perhaps less
242 clear. Alsea salt marshes have room for expansion onto tidal flats and subtidal regions of the bay
243 and much of its edges are in protected areas. Indeed, the morphology of Alsea Bay is similar to

244 that of Nehalem and both systems receive similarly high net fluvial sediment inputs relative to
245 estuary areas. A major difference in these systems is the rate of relative sea level rise, which is
246 low in Nehalem but relatively high in Alsea ($0.9 \pm 1.0 \text{ mm y}^{-1}$ vs $2.8 \pm 0.8 \text{ mm y}^{-1}$; Table 1), and
247 relatedly, Nehalem salt marsh has been vertically accreting at a pace ($2.9 \pm 1.0 \text{ mm y}^{-1}$)
248 exceeding the rate of relative sea level rise while Alsea has not been keeping up with sea level
249 rise, i.e., it is drowning ($1.7 \pm 0.4 \text{ mm y}^{-1}$; Peck et al., 2020). Thus, a filled vertical
250 accommodation space appears necessary for lateral expansion. In this way, the salt marsh edge
251 geometry (whether the edge is a ramp or a step) may influence lateral expansion as a ramped
252 edge is both indicative of and more conducive to expansion and a stepped edge of contraction
253 (Goodwin & Mudd, 2020). While distinguishing ramped and stepped edges in aerial photography
254 is difficult, others have noted these edge types as dominant features of Nehalem and Alsea,
255 respectively. For instance, Nehalem added much of its area over the past ~80 y through growth of
256 small (< 2 m diameter), circular, vegetated islands (termed “fairy circles”; Zhao et al., 2021) that
257 eventually became incorporated into the prograding, ramped edge (Johannessen, 1964).
258 Conversely, salt marsh edges in Alsea have been described as very steep and actively eroding
259 (Dicken, 1961; Brophy, 1999). Others have observed linkages between lateral and vertical marsh
260 morphology, though relatively less is understood about mechanisms and feedbacks driving three-
261 dimensional growth/loss in sediment-rich systems (Ganju et al., 2020), characteristic of the
262 Oregon coast.

263 A potential additional driver of intra-estuary edge contraction is wind wave attack (e.g.,
264 Fagherazzi et al., 2006; Marani et al., 2011). Most estuaries in Oregon have relatively short
265 fetches (e.g., Salmon and Coquille) or salt marsh edges that are predominately oriented away
266 from dominant oncoming winds (Figure 3A) from the SSW in Winter, NNW in Summer (e.g.,

267 Netarts), and are therefore likely less subject to wind-wave attack. However, when fetch is
268 relatively long (up to 4 km), edges perpendicular to oncoming winter winds experience less
269 expansion (Nehalem; Figure 3B) and more contraction (Alsea; Figure 3C) on average than other
270 salt marsh edges, though neither of these rates are significantly different when compared to
271 protected edges. Interestingly, in these same estuaries, edges perpendicular to oncoming
272 northwesterly summer winds experience more expansion than other edges. Future field
273 monitoring should investigate this; however, it is possible that summer wind waves redistribute
274 estuarine sediment towards these edges resulting in growth. Regardless, both salt marshes have a
275 smaller fraction of their edges perpendicular to oncoming summer winds than winter winds.
276 Thus, winter wind is a greater erosive force than summer wind despite displaying similar speeds
277 (Figure 3A), possibly because of increased water levels from fluvial discharge, onshore Ekman
278 transport (Komar et al., 2011), and storm surge due to atmospheric rivers (Khouakhi & Villarini,
279 2016). Overall, however, wave attack due to strong winds does not appear to be a first order
280 control on salt marsh edge change in Oregon estuaries given that few estuaries have long fetches
281 and exposed areas do not generally experience more erosion than protected areas. The majority
282 of edge contraction may be a product of fluvial discharge creating high velocity flows and
283 weaker and more consistent wave attack, as has been observed elsewhere (Leonardi, Defne, et
284 al., 2016; Leonardi, Ganju, et al., 2016).



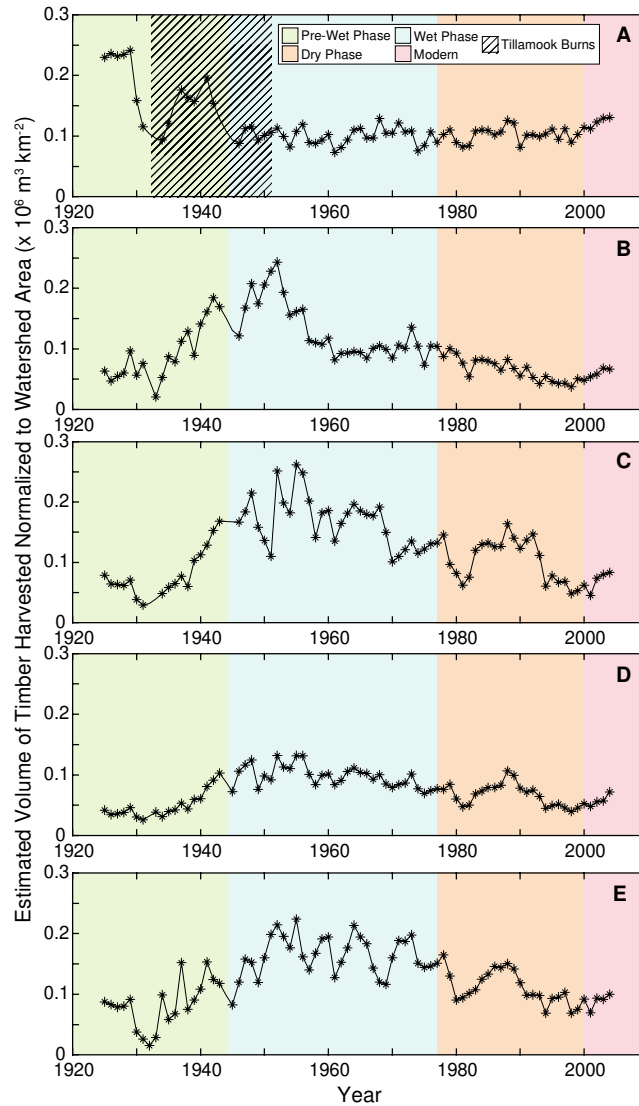
285
 286 **Figure 3.** (a) Wind rose displaying the frequency (displayed as percent values that increase with
 287 each concentric gray circle) of wind speeds (displayed as colors from 10 m s⁻¹ as white to greater
 288 than 30 m s⁻¹ as dark gray) from differing directions (displayed as degrees on the circle) for long-
 289 term (≥ 15 y) stations along the Oregon coast. Red and blue shaded directions are predominately
 290 summer (April to October) and winter (November to March) months, respectively. (b-c)
 291 Nehalem and Alsea mean rates of edge change for edges protected from wind and exposed to
 292 winter and summer winds (note difference in y axis). Rates are normalized to the fraction of edge
 293 lengths of interest divided by the total edge length. Bars indicate standard deviations.

294 *4.2 Temporal controls on lateral expansion & contraction*

295 Rates of salt marsh lateral expansion and contraction varied significantly over the last
 296 ~80 y and were divided into four general periods (1939 to 1944, 1944 to 1977, 1977 to 2000, and
 297 2000 to 2018; Figure 2) based on available aerial photographs and dominant forcings to assess
 298 the influences of changing land use and hydroclimate.

299 *4.2.1 1939 to 1944*

300 From 1939 to 1944, timber harvest and associated activities (e.g., clearcutting and road
301 construction) began to intensify (Andrews & Kutara, 2005; Figure 4) and as a result, sediment
302 supply was likely elevated. Removal of forest vegetation, especially from the steep terrain of the
303 Oregon Coast Range, destabilizes slopes and accelerates sediment erosion, though there is a lag
304 time related to root decay (~ 5 y) and a large precipitation event is frequently required to initiate
305 mass movement (Swanston & Swanson, 1976). Log drives often accompanied by splash
306 damming (facilitation of downstream transport of timber accumulated behind a dam by
307 dynamiting) in the early half of the 20th century were common in Nehalem and Coquille; splash
308 damming increased both the magnitude and frequency of discharge events, elevating sediment
309 transport (Miller, 2010). Parts of the Nehalem basin were also influenced by the Tillamook
310 Burns, a series of wildfires that burned ~1,400 km² of old growth forest in the Nehalem and
311 adjacent basins from 1933 to 1951, further elevating downstream sediment delivery (Komar et
312 al., 2004). Unfortunately, estimating the exact (per basin or per decade) impact of logging on
313 sediment flux along the Oregon coast is nearly impossible because of the poor stream gauge data
314 in most of the Coast Range; lack of timber harvest records beyond total volume per county (i.e.,
315 coarse spatial resolution); lag times between harvest, root decay, and slope destabilization; and
316 indirect relationship between slope destabilization and sediment transport. Regardless, the
317 general relationship between increased sediment flux and logging has been established both in a
318 small Oregon coastal basin as part of the Alsea Watershed Study (Beschta & Jackson, 2008) and
319 in similar geographic areas, such as Northern California, which have better stream gauge records
320 (Sommerfield & Wheatcroft, 2007; Warrick et al., 2013).



321

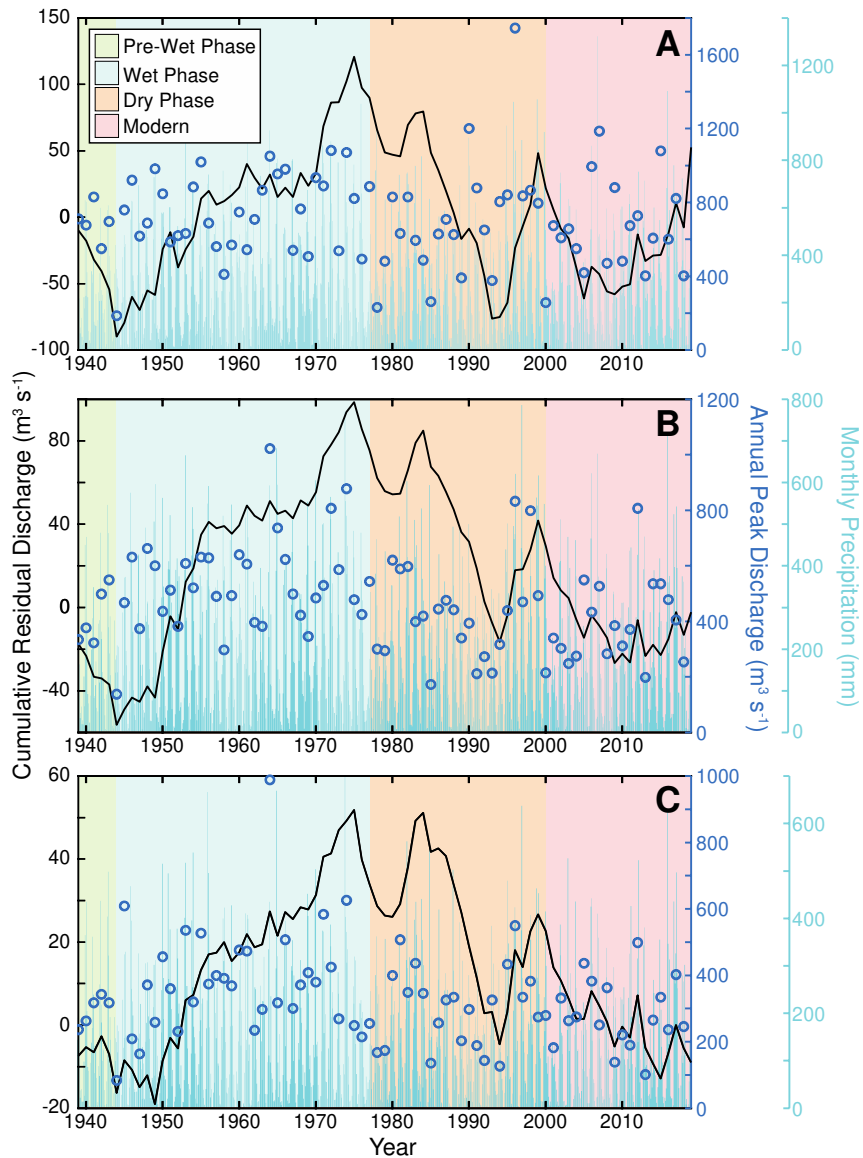
322 **Figure 4.** Volume (i.e., board feet) of timber harvested estimated for and normalized to each
 323 watershed (a-e: Nehalem, Netarts, Salmon, Alsea, & Coquille) based on county-specific timber
 324 harvest data (Andrews & Kutara, 2005) and the fraction of basin area within each county. The
 325 blue box indicates the wet phase of the Pacific Decadal Oscillation, which coincides with peak
 326 harvest in most basins, except Nehalem which was recovering from the Tillamook Burns (1933
 327 to 1951).

328 Likely as a result of their histories of logging, Nehalem and Coquille salt marshes
 329 displayed their fastest expansion rates from 1939 to 1944 (Figure 2b). Despite the short period

330 over which rates could be calculated (5 y), the overall addition to salt marsh area was still
331 sizeable in both systems (Figure 2a). Additionally, given that intensive logging was widespread
332 during this period but Netarts and Alsea both did not display growth, and indeed Alsea
333 experienced area loss, the rapid expansion of Nehalem and Coquille could be a result of the
334 particularly destructive splash damming that occurred in those watersheds prior to the study
335 period (last known dates were 1928 and 1925 in Nehalem and Coquille, respectively; Miller,
336 2010). Moreover, Nehalem's rate of area gain may have been particularly high due to excess
337 sediment supplied by the Tillamook Burns.

338 *4.2.2 1944 to 1977*

339 The next period, 1944 to 1977, was characterized by conditions that favored high fluvial
340 suspended sediment loads during the wet phase of the PDO combined with increased sediment
341 erosion due to maximal timber harvests in the 1950s (Andrews & Kutara, 2005; Figure 4) that
342 continued to utilize destructive logging methods (Hatten et al., 2018; Richardson et al., 2018).
343 The wet phase of the PDO coincides with more precipitation and numerous large storm events
344 (evident in elevated cumulative residual discharge; Figure 5), including the December 1964
345 flood (Wheatcroft et al., 2013), the largest flood on record for numerous Oregon coastal rivers
346 (St. George & Mudelsee, 2019).



347

348 **Figure 5.** Cumulative residual discharge (left, black y-axis, solid line; note different y-axes
 349 scales), peak discharge (first right, dark blue y-axis, open circles; note different y-axes scales),
 350 and monthly precipitation (second right, light blue y-axis, bars; note different y-axes scales) from
 351 1939 to the present for the **(a-c):** Nehalem, Alsea, and Coquille Rivers. Note: the Coquille gauge
 352 is located in the river headwaters (drainage area = 440 km²).

353 During this period, all salt marshes displayed growth, even the systems with net neutral
354 or negative lateral change rates calculated over the ~80 y record of aerial photographs (Figure 2).
355 Netarts, with its limited natural suspended sediment supply ($2.6 \times 10^3 \text{ t km}^{-2} \text{ y}^{-1}$), added 2.5 ha.
356 Furthermore, Salmon salt marshes also displayed growth, though slight, despite its limited space
357 for expansion. Perhaps most surprising, Alsea grew 3.5 ha though displaying contraction during
358 all other time periods. The fastest growth rate was observed in Nehalem, resulting in the largest
359 area gain (46 ha) over the last ~80 y. Although Coquille also experienced expansion, the rate was
360 lower than the previous period. While the reason for this result is unclear, it could be related to
361 increased channel edge erosion (Figure S1) resulted from increased discharge during the wet
362 phase (Figure 5C). This may be especially important in Coquille, which has the largest watershed
363 of our study sites (Table 1) and thus the greatest mean annual discharge. Additionally, cessation
364 of splash damming two decades prior, which had been particularly prevalent in the Coquille
365 basin (Miller, 2010), may have resulted in relatively less sediment transport from 1944 to 1977
366 despite increased logging.

367 Similar patterns of mid-century elevated sediment accumulation have been observed in
368 Oregon Coast Range lake sediments (Richardson et al., 2018; Wetherell et al., 2021) and in
369 continental shelf records (Wheatcroft et al., 2013), indicating preservation of the logging/wet
370 phase signal along the sediment routing system. Unfortunately, however, disentangling the
371 relative influences of logging and related activities (e.g., wildfire, road construction) from natural
372 precipitation/discharge events on sediment flux and storage along the Oregon margin remains
373 elusive given their coincidence and the coarseness of timber harvest data relative to precipitation
374 and runoff metrics.

375 *4.2.3 1977 to 2000*

376 From 1977 to 2000 sediment supplies waned (Hatten et al., 2018; Richardson et al., 2018;
377 Wetherell et al., 2021), a combined result of decreased cumulative residual discharges during the
378 dry phase of the PDO (Figure 5) and both declining timber harvests (Andrews & Kutara, 2005;
379 Figure 4) and improvement in timber practices. Various forest management acts (such as The
380 Oregon Forest Practices Act and Rules first passed in 1971; ODF, 1994) were aimed at reducing
381 erosion via numerous methods including the creation of riparian buffers; enforcement of
382 reforestation; improvement in extraction methods and road positioning; and reduction in clear-
383 cutting.

384 Likely related to these conditions favoring reduced sediment supply, lateral expansion
385 rates slowed (Nehalem and Netarts) or reversed to net contraction (Salmon and Alsea) during
386 this period in all estuaries except Coquille (Figure 2). Coquille experienced modest salt marsh
387 growth during the dry phase, highlighting the complexity of morphodynamic responses. As most
388 of the edge contraction in Coquille is along the channel edge and therefore likely a result of high
389 velocity discharge, spatially integrated area expansion during the dry phase could be a result of
390 reduced discharge. As additional evidence, Coquille displayed the opposite pattern – somewhat
391 diminished rates of expansion under higher discharge conditions – during the wet phase.

392 *4.2.4 2000 to 2018*

393 From 2000 to 2018, the PDO switched between wet and dry phases on short time periods,
394 cumulative residual discharges have remained relatively constant indicating neither elevated nor
395 low discharges (Figure 5), and contemporary timber harvest methods have had little impact on
396 suspended sediment yields (Hatten et al., 2018). During this modern period all salt marshes have
397 displayed lateral contraction except for Nehalem, in which rates slowed but were not negative

398 (Figure 2). The reason for these trends is unclear though it may be part of the continued
399 contraction of the salt marsh platforms from sizes made unsustainably large during the previous
400 decades of higher sediment flux. Others have observed similar trends of rapid vegetated intertidal
401 expansion followed by periods of contraction on multi-decadal/centennial timescales due to
402 changes in land-use practices (deforestation, reforestation, and damming) that influence fluvial
403 sediment delivery along the US East Coast (e.g., Ward et al., 1998), coast of New Zealand (e.g.,
404 Nichol et al., 2000; Pasternack et al., 2001; Kirwan et al., 2011), and coast of China (e.g., Yang
405 et al., 2002). Rapid growth during the early and mid-halves of the 20th century may have actually
406 promoted recent edge contraction, as steepening of the marsh boundary during progradation can
407 result in vegetation collapse and marsh edge retreat (van de Koppel et al., 2005), and significant
408 elevation differences between an accreting vegetated platform and adjacent tidal flat may
409 enhance instability and thus erosion (Bouma et al., 2016; Schuerch et al., 2019).

410 Other explanations for contraction of Oregon salt marshes include increased storminess
411 and/or accelerated sea level rise. While there is little evidence in the tide gauge record for
412 increased sea level rise off the coast of Oregon over recent decades (Boon & Mitchell, 2015),
413 offshore wind speeds have increased in the Northeast Pacific (Gower, 2002) and average winter
414 significant wave heights offshore have increased since the mid-1970s (Allan & Komar, 2006;
415 Ruggiero et al., 2010), perhaps having resulted in increased water levels and wave-driven edge
416 contraction inside the bays.

417 *4.2.4 Future & insights*

418 If current trajectories of edge change persist, Oregon salt marshes will continue to
419 contract. It is possible that gains in salt marsh area during the mid-20st century may be lost
420 assuming no significant increase in fluvial suspended sediment due to intensive land-use and/or

421 wetter climatic conditions. Further, total water levels within Oregon estuaries are generally
422 expected to increase into the future because of climate impacts on sea level, wind waves, and
423 discharge (Cheng et al., 2015). Given the potential for accelerations in climate change, especially
424 relative sea level rise, the rate of area loss may dramatically increase.

425 On short time periods (decadal to multidecadal), these results highlight the importance of
426 sediment supply on salt marsh lateral growth. Increases in sediment delivery to the marsh
427 platform through changes in hydroclimate and/or land use can spur periods of growth even in
428 systems that already have high sediment loads (as in the cases of Nehalem and Coquille) and/or
429 conditions that might not favor growth (as in the cases of Salmon and Alsea). However, on
430 longer time periods (~80 y) high sediment supplies, whether natural or anthropogenic, do not
431 always result in net progradation in estuaries without substantial tidal flat or subtidal area for
432 expansion (e.g., Salmon) and in estuaries without a filled vertical accommodation space due to
433 relatively high rates of sea level rise (e.g., Alsea). Others have noted the importance of sediment
434 supply on salt marsh expansion (e.g., Ladd et al., 2019), but the spatially diverse and temporally
435 dynamic nature of the Oregon coast highlights the complexities of salt marsh morphodynamics
436 and need for more observations from understudied regions (Wiberg et al., 2020). Ultimately,
437 both short-term (decadal to multi-decadal) and long-term (multi-decadal to centennial)
438 observations of lateral change are valuable to understanding the individual and cumulative
439 impacts of the various drivers on salt marsh morphology, critical for predicting future resilience
440 under accelerating climate change and shifting land use.

441 **5 Conclusions**

442 These results provide insight into net lateral rates of salt marsh expansion/contraction for
443 an understudied but significant portion of the US coastline. Moreover, in addition to highlighting

444 the complexity of Oregon intertidal morphodynamics, these results are applicable to other salt
445 marshes globally, indicating that:

446 (1) Regardless of spatially integrated rates of salt marsh lateral change, long-term
447 expansion occurs along protected marsh edges where water velocities slacken, whereas
448 contraction occurs along exposed marsh edges where channel velocities are highest. In some
449 systems, as is the case in Oregon estuaries, wave attack due to strong winds may not always be a
450 first order control on salt marsh contraction; rather, fluvial discharge creating high velocity flows
451 and weaker and more consistent wave attack may be more important controlling factors.

452 (2) Marshes will exhibit net lateral expansion when there exists room for growth onto
453 unvegetated tidal flats, vertical accommodation space has been filled, and relatively high
454 sediment supply.

455 (3) Salt marsh expansion/contraction can be relatively rapid, switching from expansion to
456 contraction on ~20 y time scales. This result highlights the need for long-term monitoring to
457 assess lateral trends as salt marshes that display short-term expansion may reverse to contraction
458 in a proceeding decade, and vice versa. Moreover, empirical studies of marsh lateral
459 expansion/contraction can help inform process-based models, critical for predicting future
460 trajectories (Fagherazzi et al., 2020).

461 (4) Temporally variable salt marsh expansion/contraction is strongly influenced by
462 changes in suspended sediment supply, which is controlled by alterations in anthropogenic land
463 use and climatic variations. As evidence, during the wet phase of the PDO, coincident with
464 intensive timber harvest, all Oregon salt marshes expanded despite numerous site-to-site
465 differences in long-term lateral change rates. Conversely, during the warm phase of the PDO,
466 concurrent with both a decrease in timber harvest magnitude and improvement of logging

467 practices, rates of expansion stabilized or reversed. It is quite possible that other systems with a
468 similar land-use history (e.g., US East Coast, New Zealand) of widespread forest clearance may
469 have had a similar salt marsh lateral trajectory of expansion followed by contraction, as other
470 have observed (e.g., Pasternack et al., 2001; Kirwan et al., 2011).

471 (5) Current trends of salt marsh contraction will likely persist into the future and may be
472 worsened by rising sea level, increased storminess, and further land management strategies that
473 reduce suspended sediment yields.

474 **Acknowledgments**

475 Research took place at Oregon State University (Corvallis, OR) in the traditional
476 homelands of the Mary's River or Ampinefu Band of Kalapuya. Following the Willamette Valley
477 Treaty of 1855, the Kalapuya people were forcibly removed to reservations in Western Oregon.
478 Today, living descendants of these people are a part of the Confederated Tribes of Grand Ronde
479 Community of Oregon and Confederated Tribes of the Siletz Indians.

480 We are grateful to the valuable suggestions provided by the peer reviewers and editors.
481 We thank Laura Brophy, Miguel Goñi, Jasmine King, Emerson Webb, and Rosemary Pazdral for
482 their feedback on earlier drafts. We thank Julia Jones for sharing her GIS expertise.

483 **Funding:** Research was funded by Oregon Sea Grant [project # NA14OAR4170064; R/HBT-21-
484 Wheatcroft]; and an NSF Research Traineeship fellowship [project # 1545188].

485 **Data Statement:** GIS data: <https://doi.org/10.4211/hs.22c662d201354961ba74e61aeca43a85>.

486 **Declaration of Competing Interest:** The authors declare no conflicts of interest.

487 **References**

- 488 Allan, J. C., & Komar, P. D. (2006). Climate controls on US West Coast erosion processes.
489 *Journal of Coastal Research*, 22(3), 511-529. <https://doi.org/10.2112/03-0108.1>
- 490 Andrews, A., & Kutara, K. (2005). Oregon's timber harvests: 1849-2004. Salem, OR: Oregon
491 Department of Forestry.
492 <https://www.oregon.gov/ODF/Documents/WorkingForests/oregonstimberharvests.pdf>
- 493 Barbier, E. B., Hacker, S. D., Kennedy, C., Koch, E. W., Stier, A. C., & Silliman, B. R. (2011).
494 The value of estuarine and coastal ecosystem services. *Ecological Monographs*, 81(2),
495 169-193. <https://doi.org/10.1890/10-1510.1>
- 496 Beschta, R. L., & Jackson, W. L. (2008). Forest practices and sediment production in the Alsea
497 Watershed Study. In J.D. Stednick (Ed), Hydrological and biological responses to forest
498 practices. Springer, New York, NY, pp. 55-66.
- 499 Benner, P. A. (1992). Historical reconstruction of the Coquille River and surrounding landscape.
500 In *Near Coastal Waters National Pilot Project: The Coquille River, Oregon*. (Action Plan
501 for Oregon Coastal Watersheds, Estuaries and Ocean Waters, 1988-91). Environmental
502 Protection Agency.
- 503 Boon, J. D., & Mitchell, M. (2015). Nonlinear change in sea level observed at North American
504 tide stations. *Journal of Coastal Research*, 31(6), 1295-1305.
505 <https://doi.org/10.2112/JCOASTRES-D-15-00041.1>
- 506 Bouma, T. J., Van Belzen, J., Balke, T., Van Dalen, J., Klaassen, P., Hartog, A. M., ... &
507 Herman, P. M. J. (2016). Short-term mudflat dynamics drive long-term cyclic salt marsh
508 dynamics. *Limnology and Oceanography*, 61(6), 2261-2275.
509 <https://doi.org/10.1002/lno.10374>

510 Brophy, L. S., & Ewald, M. J. (2017). Modeling sea level rise impacts to Oregon's tidal
511 wetlands: Maps and prioritization tools to help plan for habitat conservation into the
512 future. (Report prepared for MidCoast Watersheds Council Newport, Oregon). Corvallis,
513 OR: Institute for Applied Ecology.

514 Brophy, L. S., Greene, C. M., Hare, V. C., Holycross, B., Lanier, A., Heady, W. N., ... & Dana,
515 R. (2019). Insights into estuary habitat loss in the western United States using a new
516 method for mapping maximum extent of tidal wetlands. *PloS One*, *14*(8), e0218558.
517 <https://doi.org/10.1371/journal.pone.0218558>

518 Brophy, L.S. (1999). Final report—Yaquina and Alsea River Basins estuarine wetland site
519 prioritization project. (Report prepared for the MidCoast Watersheds Council, Newport,
520 Oregon). Corvallis, OR: Green Point Consulting.

521 Burgette, R. J., Weldon, R. J., & Schmidt, D. A. (2009). Interseismic uplift rates for western
522 Oregon and along-strike variation in locking on the Cascadia subduction zone. *Journal of*
523 *Geophysical Research: Solid Earth*, *114*, B01408. <https://doi.org/10.1029/2008JB005679>

524 Carr, S. J., Diggins, L. M., & Spencer, K. L. (2020). There is no such thing as 'undisturbed' soil
525 and sediment sampling: sampler-induced deformation of salt marsh sediments revealed
526 by 3D X-ray computed tomography. *Journal of Soils and Sediments*, *20*, 2960-2976.
527 <https://doi.org/10.1007/s11368-020-02655-7>

528 Cheng, T. K., Hill, D. F., Beamer, J., & García-Medina, G. (2015). Climate change impacts on
529 wave and surge processes in a Pacific Northwest (USA) estuary. *Journal of Geophysical*
530 *Research: Oceans*, *120*(1), 182-200. <https://doi.org/10.1002/2014JC010268>

531 Daly, C., Neilson, R. P., & Phillips, D. L. (1994). A statistical-topographic model for mapping
532 climatological precipitation over mountainous terrain. *Journal of Applied Meteorology*

533 *and Climatology*, 33(2), 140-158. [https://doi.org/ 10.1175/1520-](https://doi.org/10.1175/1520-)
534 0450(1994)033<0140:ASTMFM>2.0.CO;2

535 Dicken, S. N. (1961). Some recent physical changes of the Oregon coast. (Report for the Office
536 of Naval Research, U.S. Department of the Navy, Contract NONR-2771(04)). Eugene,
537 OR: Department of Geography, University of Oregon.

538 Fagherazzi, S., Carniello, L., D'Alpaos, L., & Defina, A. (2006). Critical bifurcation of shallow
539 microtidal landforms in tidal flats and salt marshes. *Proceedings of the National Academy*
540 *of Sciences*, 103(22), 8337-8341. <https://doi.org/10.1073/pnas.0508379103>

541 Fagherazzi, S., Mariotti, G., Leonardi, N., Canestrelli, A., Nardin, W., & Kearney, W. S. (2020).
542 Salt marsh dynamics in a period of accelerated sea level rise. *Journal of Geophysical*
543 *Research: Earth Surface*, 125(8), e2019JF005200. <https://doi.org/10.1029/2019JF005200>

544 Ganju, N. K., Defne, Z., & Fagherazzi, S. (2020). Are elevation and open-water conversion of
545 salt marshes connected? *Geophysical Research Letters*, 47(3), e2019GL086703.
546 <https://doi.org/10.1029/2019GL086703>

547 Gedan, K. B., Silliman, B. R., & Bertness, M. D. (2009). Centuries of human-driven change in
548 salt marsh ecosystems. *Annual Review of Marine Science*, 1, 117-141.
549 <https://doi.org/10.1146/annurev.marine.010908.163930>

550 Goodwin, G. C., & Mudd, S. M. (2020). Detecting the Morphology of Prograding and Retreating
551 Marsh Margins—Example of a Mega-Tidal Bay. *Remote Sensing*, 12(1), 13.
552 <https://doi.org/10.3390/rs12010013>

553 Gower, J. F. R. (2002). Temperature, wind and wave climatologies, and trends from marine
554 meteorological buoys in the northeast Pacific. *Journal of Climate*, 15(24), 3709-3718.
555 [https://doi.org/10.1175/1520-0442\(2002\)015<3709:TWAWCA>2.0.CO;2](https://doi.org/10.1175/1520-0442(2002)015<3709:TWAWCA>2.0.CO;2)

556 Hatten, J. A., Segura, C., Bladon, K. D., Hale, V. C., Ice, G. G., & Stednick, J. D. (2018). Effects
557 of contemporary forest harvesting on suspended sediment in the Oregon Coast Range:
558 Alsea Watershed Study Revisited. *Forest Ecology and Management*, 408, 238-248.
559 <https://doi.org/10.1016/j.foreco.2017.10.049>

560 Himmelstoss, E. A., Henderson, R. E., Kratzmann, M. G., & Farris, A. S. (2018). Digital
561 shoreline analysis system (DSAS) version 5.0 user guide. (Open-File Report 2018-1179).
562 Reston, VA: US Geological Survey.

563 Johannessen, C. L. (1964). Marshes prograding in Oregon: aerial photographs. *Science*,
564 146(3651). 1575-1578. <https://doi.org/10.1126/science.146.3651.1575>

565 Khouakhi, A., & Villarini, G. (2016). On the relationship between atmospheric rivers and high
566 sea water levels along the US West Coast. *Geophysical Research Letters*, 43(16), 8815-
567 8822. <https://doi.org/10.1002/2016GL070086>

568 Kirwan, M. L., Murray, A. B., Donnelly, J. P., & Corbett, D. R. (2011). Rapid wetland expansion
569 during European settlement and its implication for marsh survival under modern
570 sediment delivery rates. *Geology*, 39(5), 507-510. <https://doi.org/10.1130/G31789.1>

571 Kirwan, M. L., Temmerman, S., Skeechn, E. E., Guntenspergen, G. R., & Fagherazzi, S. (2016).
572 Overestimation of marsh vulnerability to sea level rise. *Nature Climate Change*, 6(3),
573 253-260. <https://doi.org/10.1038/nclimate2909>

574 Kirwan, M. L., Walters, D. C., Reay, W. G., & Carr, J. A. (2016). Sea level driven marsh
575 expansion in a coupled model of marsh erosion and migration. *Geophysical Research*
576 *Letters*, 43(9), 4366-4373. <https://doi.org/10.1002/2016GL068507>

577 Komar, P. D., Allan, J. C., & Ruggiero, P. (2011). Sea level variations along the US Pacific
578 Northwest coast: Tectonic and climate controls. *Journal of Coastal Research*, 27(5), 808-
579 823. <https://doi.org/10.2112/JCOASTRES-D-10-00116.1>

580 Komar, P. D., McManus, J., & Styllas, M. (2004). Sediment accumulation in Tillamook Bay,
581 Oregon: natural processes versus human impacts. *Journal of Geology*, 112(4), 455-469.
582 <https://doi.org/10.1086/421074>

583 Ladd, C. J., Duggan-Edwards, M. F., Bouma, T. J., Pagès, J. F., & Skov, M. W. (2019).
584 Sediment supply explains long-term and large-scale patterns in salt marsh lateral
585 expansion and erosion. *Geophysical Research Letters*, 46(20), 11178-11187.
586 <https://doi.org/10.1029/2019GL083315>

587 Langston, A. K., Durán Vinent, O., Herbert, E. R., & Kirwan, M. L. (2020). Modeling long-term
588 salt marsh response to sea level rise in the sediment-deficient Plum Island Estuary,
589 MA. *Limnology and Oceanography*, 65(9), 2142-2157. <https://doi.org/10.1002/lno.11444>

590 Leonardi, N., Defne, Z., Ganju, N. K., & Fagherazzi, S. (2016). Salt marsh erosion rates and
591 boundary features in a shallow Bay. *Journal of Geophysical Research: Earth Surface*,
592 121(10), 1861-1875. <https://doi.org/10.1002/2016JF003975>

593 Leonardi, N., Ganju, N. K., & Fagherazzi, S. (2016). A linear relationship between wave power
594 and erosion determines salt-marsh resilience to violent storms and hurricanes.
595 *Proceedings of the National Academy of Sciences*, 113(1), 64-68.
596 <https://doi.org/10.1073/pnas.1510095112>

597 Marani, M., D'Alpaos, A., Lanzoni, S., & Santalucia, M. (2011). Understanding and predicting
598 wave erosion of marsh edges. *Geophysical Research Letters*, 38(21).
599 <https://doi.org/10.1029/2011GL048995>

600 Mariotti, G., & Carr, J. (2014). Dual role of salt marsh retreat: Long-term loss and short-term
601 resilience. *Water Resources Research*, 50(4), 2963-2974.
602 <https://doi.org/10.1002/2013WR014676>

603 Mariotti, G., & Fagherazzi, S. (2010). A numerical model for the coupled long-term evolution of
604 salt marshes and tidal flats. *Journal of Geophysical Research: Earth Surface*, 115(F1).
605 <https://doi.org/10.1029/2009JF001326>

606 Mazzotti, S., Jones, C., & Thomson, R. E. (2008). Relative and absolute sea level rise in western
607 Canada and northwestern United States from a combined tide gauge-GPS
608 analysis. *Journal of Geophysical Research: Oceans*, 113, C11019.
609 <https://doi.org/10.1029/2008JC004835>

610 Miller, R. R. (2010). Is the Past Present? Historical Splash-dam Mapping and Stream
611 Disturbance Detection in the Oregon Coastal Province, (Masters Thesis). Retrieved from
612 Oregon State University Library
613 (https://ir.library.oregonstate.edu/concern/graduate_thesis_or_dissertations/4m90f001t).
614 Oregon State University. Corvallis, OR: Oregon State University.

615 Molino, G. D., Defne, Z., Aretxabaleta, A. L., Ganju, N. K., & Carr, J. A. (2021). Quantifying
616 Slopes as a Driver of Forest to Marsh Conversion Using Geospatial Techniques:
617 Application to Chesapeake Bay Coastal-Plain, United States. *Frontiers in Environmental*
618 *Science*, 9, 149. <https://doi.org/10.3389/fenvs.2021.616319>

619 Nichol, S. L., Augustinus, P. C., Gregory, M. R., Creese, R., & Horrocks, M. (2000).
620 Geomorphic and sedimentary evidence of human impact on the New Zealand coastal
621 landscape. *Physical Geography*, 21(2), 109-132.
622 <https://doi.org/10.1080/02723646.2000.10642702>

623 Oregon Department of Forestry (ODF). (1994). The Oregon Forest Practices Act Water
624 Protection Rules: Scientific and Policy Considerations. ODF, Salem, OR, p. 66.

625 Pasternack, G. B., Brush, G. S., & Hilgartner, W. B. (2001). Impact of historic land-use change
626 on sediment delivery to a Chesapeake Bay subestuarine delta. *Earth Surface Processes
627 and Landforms*, 26(4), 409-427.

628 Peck, E. K., Wheatcroft, R. A., & Brophy, L. S. (2020). Controls on sediment accretion and blue
629 carbon burial in tidal saline wetlands: Insights from the Oregon coast, USA. *Journal of
630 Geophysical Research: Biogeosciences*, 125(2), e2019JG005464.
631 <https://doi.org/10.1029/2019JG005464>

632 PRISM Climate Group, Oregon State University, <https://prism.oregonstate.edu>, data created 4
633 Feb 2014 (accessed 11 Feb 2022).

634 Redfield, A. C. (1972). Development of a New England salt marsh. *Ecological monographs*,
635 42(2), 201-237. <https://doi.org/10.2307/1942263>

636 Richardson, K. N. D., Hatten, J. A., & Wheatcroft, R. A. (2018). 1500 years of lake
637 sedimentation due to fire, earthquakes, floods and land clearance in the Oregon Coast
638 Range: Geomorphic sensitivity to floods during timber harvest period. *Earth Surface
639 Processes and Landforms*, 43(7), 1496-1517. <https://doi.org/10.1002/esp.4335>

640 Ruggiero, P., Komar, P. D., & Allan, J. C. (2010). Increasing wave heights and extreme value
641 projections: The wave climate of the US Pacific Northwest. *Coastal Engineering*, 57(5),
642 539-552. <https://doi.org/10.1016/j.coastaleng.2009.12.005>

643 Ruggiero, P., Kratzmann, M. G., Himmelstoss, E. A., Reid, D., Allan, J., & Kaminsky, G.
644 (2013). National assessment of shoreline change: historical shoreline change along the

645 Pacific Northwest coast. (Open-File Report 2012-1007). Reston, VA: US Geological
646 Survey.

647 Schieder, N. W., Walters, D. C., & Kirwan, M. L. (2018). Massive upland to wetland conversion
648 compensated for historical marsh loss in Chesapeake Bay, USA. *Estuaries and Coasts*,
649 *41*(4), 940-951. <https://doi.org/10.1007/s12237-017-0336-9>

650 Schuerch, M., Spencer, T., & Evans, B. (2019). Coupling between tidal mudflats and salt
651 marshes affects marsh morphology. *Marine Geology*, *412*, 95-106.
652 <https://doi.org/10.1016/j.margeo.2019.03.008>

653 Sommerfield, C. K., & Wheatcroft, R. A. (2007). Late Holocene sediment accumulation on the
654 northern California shelf: Oceanic, fluvial, and anthropogenic influences. *Geological*
655 *Society of America Bulletin*, *119*(9-10), 1120-1134. <https://doi.org/10.1130/B26019.1>

656 St. George, S., & Mudelsee, M. (2019). The weight of the flood-of-record in flood frequency
657 analysis. *Journal of Flood Risk Management*, *12*, e12512.
658 <https://doi.org/10.1111/jfr3.12512>

659 Swanston, D.N., & Swanson, E.J. (1976). Timber harvesting, mass erosion, and steepland forest
660 geomorphology in the Pacific Northwest. In: Coates D.R. (Ed), *Geomorphology and*
661 *engineering*. Dowden, Hutchinson and Ross, Inc., Stroudsburg, Pa., pp. 199–221.

662 Thorne, K., MacDonald, G., Guntenspergen, G., Ambrose, R., Buffington, K., Dugger, B., ... &
663 Takekawa, J. (2018). US Pacific coastal wetland resilience and vulnerability to sea-level
664 rise. *Science Advances*, *4*(2), eaao3270. <https://doi.org/10.1126/sciadv.aao3270>

665 van de Koppel, J., Wal, D. V. D., Bakker, J. P., & Herman, P. M. (2005). Self-organization and
666 vegetation collapse in salt marsh ecosystems. *The American Naturalist*, *165*(1), E1-E12.
667 <https://doi.org/10.1086/426602>

668 Ward, L. G., Kearney, M. S., & Stevenson, J. C. (1998). Variations in sedimentary environments
669 and accretionary patterns in estuarine marshes undergoing rapid submergence,
670 Chesapeake Bay. *Marine Geology*, *151*(1-4), 111-134. [https://doi.org/10.1016/S0025-](https://doi.org/10.1016/S0025-3227(98)00056-5)
671 [3227\(98\)00056-5](https://doi.org/10.1016/S0025-3227(98)00056-5)

672 Warrick, J. A., Madej, M. A., Goñi, M. A., & Wheatcroft, R. A. (2013). Trends in the
673 suspended-sediment yields of coastal rivers of northern California, 1955–2010. *Journal*
674 *of Hydrology*, *489*, 108-123. <https://doi.org/10.1016/j.jhydrol.2013.02.041>

675 Weston, N. B. (2014). Declining sediments and rising seas: an unfortunate convergence for tidal
676 wetlands. *Estuaries and Coasts*, *37*(1), 1-23. <https://doi.org/10.1007/s12237-013-9654-8>

677 Wetherell, L. R., Ely, L. L., Roering, J. J., Walsh, M. K., Burchfield, M. J., Nace, K. E., ... &
678 Struble, W. T. (2021). Quantifying sedimentation patterns of small landslide-dammed
679 lakes in the central Oregon coast range. *Earth Surface Processes and Landforms* (*46*)7, 1-
680 18. <https://doi.org/10.1002/esp.5106>

681 Wheatcroft, R. A., Goñi, M. A., Richardson, K. N., & Borgeld, J. C. (2013). Natural and human
682 impacts on centennial sediment accumulation patterns on the Umpqua River margin,
683 Oregon. *Marine Geology*, *339*(1), 44-56. <https://doi.org/10.1016/j.margeo.2013.04.015>

684 Wiberg, P. L., Fagherazzi, S., & Kirwan, M. L. (2020). Improving predictions of salt marsh
685 evolution through better integration of data and models. *Annual review of marine*
686 *science*, *12*, 389-413. <https://doi.org/10.1146/annurev-marine-010419-010610>

687 Wise, D. R. (2018). Updates to the suspended sediment SPARROW model developed for
688 western Oregon and northwestern California. (Scientific Investigations Report 2018-
689 5156). Reston, VA: US Geological Survey.

690 Yang, S. L., Zhao, Q. Y., & Belkin, I. M. (2002). Temporal variation in the sediment load of the
691 Yangtze River and the influences of human activities. *Journal of Hydrology*, 263(1-4),
692 56-71. [https://doi.org/10.1016/S0022-1694\(02\)00028-8](https://doi.org/10.1016/S0022-1694(02)00028-8)

693 Zhao, L. X., Zhang, K., Siteur, K., Li, X. Z., Liu, Q. X., & van de Koppel, J. (2021). Fairy circles
694 reveal the resilience of self-organized salt marshes. *Science Advances*, 7(6), eabe1100.
695 <https://doi.org/10.1126/sciadv.abe1100>